Arabian Journal of Chemistry (2018) **11**, 48–61

King Saud University

Arabian Journal of Chemistry

www.ksu.edu.sa
www.sciencedirect.com

ORIGINAL ARTICLE

Nanobiotechnology approach using plant rooting hormone synthesized silver nanoparticle as "nanobullets" for the dynamic applications in horticulture – An *in vitro* and *ex vitro* study

Raja Muthuramalingam Thangavelu, Dharanivasan Gunasekaran, Michael Immanuel Jesse, Mohammed Riyaz S.U, Deepan Sundarajan, Kathiravan Krishnan *

Nanobiotechnology Research Laboratory, Department of Biotechnology, University of Madras, Tamil Nadu 600 025, India

Received 9 July 2016; accepted 25 September 2016
Available online 5 October 2016

KEYWORDS

Nanobiotechnology;
Horticulture;
Hormone capped silver nanoparticles;
Target delivery;
Rooting enhancer;
Antimicrobial

Abstract Horticulture is the branch of agriculture that deals with science and technology and business of plant cultivation and it is considered to be the foremost part of the world economy. Even though, one of the major challenges which has seriously influenced the economic loss of horticulture is rooting of cuttings and root growth inhibiting plant pathogens. To address this issue through nanobiotechnology, we ingeniously build a concept of silver nanoparticles (AgNPs) as "nanobullets" can act for a dual mode like root enhancer and pathogen destroyer on the target site. After that, we succeeded in AgNPs synthesis, using two auxin rooting hormones of Indole-3-acetic acid and Indole-3-butyric acid as a reducing cum stabilizing agent. Further, its efficacy of root promoting and pathogen inhibitory action was sufficiently validated through *in vitro* and *ex vitro* studies with model plants and plant pathogens. As a result, the action duality of hormone-stabilized AgNPs was manifested to threefold enhanced root growth compared to controls and it increased the rooting capabilities against root growth inhibiting phytopathogens. This feature was also proved by the direct antifungal assay. Moreover, hormone-AgNPs left no toxicity to treated plants which was

Abbreviations: IAA, Indole-3 Acetic Acid; IBA, Indole-3-Butyric Acid; $AgNO_3$, silver nitrate; AgNPs, silver nanoparticles; AgIAA, Indole-3, Acetic Acid capped silver nanoparticles; AgIBA, Indole-3-Butyric Acid silver nanoparticles; MS, Murashige and Skoog; RAPD, random amplified polymorphic DNA; TGA, Thermogravimetric Analysis; TEM, transmission electron microscopy; SEM, scanning electron microscopy; EDS, Energy dispersive X-ray spectroscopy; FTIR, Fourier Transform Infrared Spectroscopy; PCR, Polymerase chain reaction

* Corresponding author.
E-mail addresses: rajarbiotech_phoenix@yahoo.com (R.M. Thangavelu), gdvasan@gmail.com (D. Gunasekaran), imma.biores@hotmail.com (M.I. Jesse), mriyaz4@gmail.com (M.R. S.U), deepanvit@gmail.com (D. Sundarajan), drkkathiravan@gmail.com (K. Krishnan).

Peer review under responsibility of King Saud University.

Production and hosting by Elsevier

http://dx.doi.org/10.1016/j.arabjc.2016.09.022

revealed by RAPD molecular markers. Therefore, with a detailed study and analysis with instruments such as Spectroscopy, TEM, Zetasizer, FTIR, Cyclic Voltammetry, Fluorescence microscopy (nanoparticles uptake), SEM coupled with EDS (bioaccumulation), TGA (grafting density) and PCR (RAPD analysis), this study can unravel the relevance, scope and current challenges at horticulture plants root development and plant disease management for the sustainable agricultural crop production.

1. Introduction

Nanobiotechnology is the biology-based, application-oriented frontier area of research in the hybrid discipline of Nanoscience and biotechnology with an equivalent contribution. In current nano dynasty, a nanomaterial of organic and inorganic origin ranging from 1 to 100 nm has one- or multi-dimensional applications in all the fields of science and technology in increasing numbers. Meanwhile, nanotechnology application to biotechnology will also leave no field untouched by its groundbreaking scientific innovations for human wellness; the agricultural industry is no exception. Basically, nanomaterials are distinguished depending on the origin: natural, incidental and engineered nanoparticles. Among these, engineered nanoparticles have received wide attention in all fields of science, including medical, materials and agriculture technology with significant socio-economical growth.

In the agriculture industry, engineered nanoparticles have been serving as "nano carrier", containing herbicides, chemicals, or genes, which target particular plant parts to release their content (Lian et al., 2012; Zakaria et al., 2015; Wu et al., 2011). Previously nanocapsules containing herbicides have been reported to effectively penetrate through cuticles and tissues, allowing the slow and constant release of the active substances (Perea de Lugue and Rubiales, 2009). Likewise, other literature describes that nano-encapsulated slow release of fertilizers has also become a trend to save fertilizer consumption and to minimize environmental pollution through precision farming (Jones, 2006). These are only a few examples from numerous research works which might open up exciting opportunities for nanobiotechnology application in agriculture. Also, application of this kind of engineered nanoparticles to plants should be considered the level of amicability before it is employed in agriculture practices. Based on a thorough literature survey, it was understood that there is only limited authentic information available to explain the biological consequence of engineered nanoparticles on treated plants. Certain reports underline the phytotoxicity of various origins of engineered nanoparticles to the plant caused by the subject of concentrations and sizes (Craig and Jason, 2011; Battke et al., 2008; Ghodake et al., 2011; Samardakiewicz and Wozny, 2005; El Sayed, 2004). At the same time, however, an equal number of studies were reported with a positive outcome of nanoparticles, which facilitate growth promoting nature to treat plant (Nair et al., 2010; Monica and Cremonini, 2009; Mariya and Mohamed, 2014; Juhel et al., 2011). In particular, compared to other nanoparticles, silver and gold nanoparticles based applications elicited beneficial results on various plant species with less and/or no toxicity (Raqual et al., 2009; Raja Muthuramalingam et al., 2015). Silver nanoparticles (AgNPs) treated leaves of *Asparagus* showed the increased content of ascorbate and chlorophyll (An et al., 2008). Similarly, AgNPs-treated common bean and corn has increased shoot and root length, leaf surface area, chlorophyll, carbohydrate and protein contents reported earlier (Salama, 2012). The gold nanoparticle has been used to induce growth and seed yield in *Brassica juncea* (Arora et al., 2012). Since then, only limited drawbacks were reported for silver and gold nanoparticles mediated toxicity, and still there is a huge scope for applying nanoscale manipulated products to agriculture use.

Horticulture, a leading sector in the field agriculture produces vegetables, nuts, fruits, flowers, trees and herbs, which covers almost 100% of the daily need by overall population in the world (Priede and Klavina, 2011). This potential sector also has some downside which leads to huge losses in this sector. Obviously, Rooting is a cornerstone of the horticulture industry where most of the horticultural and forestry plants are developed at tissue culture laboratories and nurseries through *in vitro* micropropagation and *ex vitro* stem-cutting technique respectively (George, 1996). Among these techniques, root development in plant cuttings is quite tedious in spite of using rooting hormones due to two main factors: different rooting abilities and root growth-deteriorating phytopathogens eventually resulting in a huge loss in horticulture (Steve Dreistadt, 2001). In order to solve these issues, a unique approach (nano-bullets) was devised to utilize the rooting hormone-stabilized silver nanoparticles both as root promoters and as antimicrobial agents in parallel. In this research work, we have used plant rooting hormones, Indole-3-Acetic Acid (IAA) and Indole-3-Butyric Acid (IBA) as a reducing cum capping agent to synthesize silver nanoparticles. And there are no reports stated nanoparticles synthesis by using plant auxin hormones previously. Both IAA and IBA are native plant growth regulators from auxin family, and specifically play a key role in root development in both *ex vitro* and *in vitro* grown plants (Becker and Hedrich, 2002; Stefancic et al., 2005; Tiberia et al., 2011). Therefore, we validated the potential of IAA- and IBA-stabilized AgNPs in enhancing root growth (*in vitro* and *ex vitro*) and antimicrobial activity (*ex vitro*) in the model plants of *Nicotiana tabacum* and *Hibiscus rosa sinensis* respectively with three destructive soil borne phytopathogens of *Curvularia lunata, Rhizoctonia solani, and Colletotrichum gloeosporioides* (Ahmed et al., 2005; John Lockwood, 1985; Khan et al., 2014). In that comprehensive study, absorption, distribution, bioaccumulation and possible phytotoxicity of hormone nanoparticles in treating plants were also examined with high throughput techniques.

2. Experimental

2.1. Reagents

Silver nitrate ($AgNO_3$) was acquired from Loba Chemie Pvt. Ltd., and Indole-3-Acetic Acid (IAA), Indole-3-Butyric Acid (IBA), MS medium components, and Potato dextrose agar were obtained from Himedia Laboratories. Sodium hypochlorite (NaClO), Agarose, Ethidium bromide, potassium bromide (KBr), glass wares and other tissue culture materials were obtained from Sisco Research Laboratories (SRL). Fungicide was (Bavistin) purchased from a local fertilizer company. PCR mixture obtained from Amplicon QIII and RAPD marker (OPK-7-5′-AGC GAG CAA G-3′) was specifically obtained from Operon Technologies, Inc., USA. Deionized water (18 $m\Omega\,cm^{-1}$) was used throughout the experiments.

2.2. Preparation of silver nanoparticles

In a typical experiment, 1 mM of silver nitrate solution was prepared by dissolving 16.9 mg of $AgNO_3$ in 100 ml of deionized water and the solution was kept in an ice bath for half an

hour. 10 mM of both IAA and IBA was prepared, separately. At the beginning of the reaction, 5 ml of 1 mM ice cold silver nitrate solutions was taken in test tubes. Then IAA and IBA solutions were separately added and mixed in test tubes containing aqueous $AgNO_3$. The time of addition of IAA and IBA in a silver nitrate solution was considered as the starting of the reaction and both mixtures were subjected to continuous stirring in a water bath at 60–70 °C until the transparent solution changed into yellow color. The color change indicates the formation of colloidal nanoparticles stabilized by IAA (at 700 µl) and IBA (at 800 µl). The IAA- and IBA-stabilized AgNPs were characterized and carried out for *in vitro* and *ex vitro* experimental studies.

2.3. Characterization of IAA- and IBA-stabilized AgNPs

Nanoparticles characterization and analysis are very essential and quite critical task using sophisticated instruments which give statistical and structural data relevant to nanoparticles shape, size, size distribution, dispersion, surface charge and their overall physiochemical properties. In this experiment, all UV-Vis spectra of AgIAA, AgIBA, $AgNO_3$ solution, water-dissolved IAA and IBA were obtained from UV-Vis Spectrometer (Shimadzu UV-1601, Japan) with UV probe 2.33 version software. Further, the IAA- and IBA-stabilized AgNPs solutions were centrifuged at 10,976*g* for 10 min in 15 °C to remove the excess stabilizing agent from the colloidal solution and residue nanoparticles were diluted in ultra-pure distilled water for further analysis. To know the nanoparticles yield, it was calculated independently according to Mie theory and some quantitative experiments from the literature with the obtained UV-Vis spectral extinction coefficient data (Trutna et al., 2008; Paramelle et al., 2014). For transmission electron microscopy analysis, IAA- and IBA-stabilized AgNPs were diluted in 1:20 ratio with deionized water to avoid overloading from which 1.5 µL was loaded with 3 mm carbon-coated copper grid and allowed to air dry at RT. Then the sample was analyzed by TEM (HITACHI H-7650, Japan) operated at an accelerating voltage of 120 kV. Here, Dynamic light scattering (DLS; Malvern Instruments Ltd., Malvern, UK) was used to determine the hydrodynamic diameter of the silver nanoparticles. All DLS measurements were performed at a fixed angle of 90° at 25 °C. The zeta potential of a particle is the overall charge that the particle acquires in a particular medium and is also measured using the same zeta size equipment at 25 °C. To know the interaction of IAA and IBA with silver nanoparticles, the solutions were subjected to FT-IR (ABB MB 3000) analysis. The sample was prepared from the pellet of IAA- and IBA-stabilized AgNPs after centrifugation at 14,000 RPM for 10 min and the pellet was grained with potassium bromide (KBr) into a fine powder. The grained powder samples were subjected to FTIR spectra analysis from 400 to 4000 cm^{-1} and the percentage of transmission was recorded and compared with the fine powders of pure IAA and IBA as the control. Cyclic voltammetry studies to comprehend the reduction of silver nanoparticles in the solution were triggered by the IAA and IBA, and change in the oxidation state of the metal ions. Cyclic voltammograms (CV) were recorded using a computer controlled 400A electrochemical analyzer using glassy carbon (GC) with 2 mm of surface diameter as working electrode, Pt wire as a counter electrode and Ag/AgCl as a reference electrode. The surface of the electrode was polished with alumina powder (0.05 µm) and rinsed carefully with double distilled water before use. Thermogravimetric Analysis (TGA) is a widely used tool for quantitative analysis of surface bound grafting densities (Benoit et al., 2012). TGA was performed with a TGA Q50 (TA instruments, New castle, Delaware). The instrument heat profile used was a heating step from 10 to 100 °C at 5 min followed by heating to 800 °C at 10 min for thermal degradation of the sample. A hormone control and AgIBA were run for TGA at gas atmosphere to determine the grafting density of hormone on silver nanoparticles which is a critical feature to consider when designing nanoparticles for biological and environmental applications.

2.4. In vitro tissue culture studies of IAA- and IBA-stabilized AgNPs

2.4.1. Plant materials and growth conditions

All the plant tissue culture experiments were conducted under defined conditions of the culture room maintained at 25 ± 2 °C, uniform light (1000 Lux) provided by fluorescent tubes over light/dark cycles of 16/8 h. The plant tissue culture-specific Murashige and Skoog (MS) medium was prepared by the standard procedure and used for explant culture (Murashige and Skoog, 1962). Media and apparatus were rendered sterile by autoclaving at 15 lbs/$in.^2$ (121 °C) for 15 min. The greenhouse-grown two months old tobacco (*Nicotiana tabacum)* plants were used as a model plant in this study. A number of 8–12 cm young stems were incised and transferred to the laboratory. From the stems, explants were cut to the length of 1.5–2 cm with one node and pre-washed in double distilled water for 10 min. Further, they were surface sterilized with 2% sodium hypochlorite for 4–5 min and then washed with sterile distilled water 3–4 times prior to the experiment. Borosil glass tubes (25 × 150 mm) each containing 15 ml of the culture medium and capped with plugs of nonabsorbent cotton were autoclaved at 120 °C for 15 min used for this experiment.

2.4.2. Application and assessment of IAA- and IBA-stabilized AgNPs through in vitro culture

The rooting ability of IAA- and IBA-stabilized AgNPs in *N. tabacum* was investigated compared with controls through *in vitro* tissue culture using MS semi-transparent medium. Initially, we have done crucial controls with $AgNO_3$ alone and along with hormone to treat *in vitro* micro cuttings. From that crucial control, we were experienced $AgNO_3$ in ionic nature in solution alone and along with hormone treated was shown toxic effects. Because it evidenced that, treated micro cuttings got severe morphological damage like burning and blackening due to silver nitrate toxicity even at 1 mM which was used for nanoparticles synthesis. The toxicity of silver to plant, in ionic condition was also reported in our previously published paper (Raja Muthuramalingam et al., 2015). Therefore, with this knowledge in hand, crucial controls were neglected throughout this study. Here the doses of test solution were fixed with concentration used in the synthesis of AgIAA and AgIBA. Such that 5 ml of both hormones stabilized silver nanoparticles solutions (0.02 mg/ml) and 5 ml of ddH_20 consisting of IAA (700 µl) and IBA (800 µl) were used for both *in vitro* and *ex vitro* experimental studies. The *N. tabacum* nodal microcut-

tings (explants) were dipped at basal end (1 in. deep) in separate 5 ml vials containing IAA-(set 'd') and IBA- (set 'e') stabilized AgNPs (approximately 0.02 mg/ml) for 30 min. In a similar way, explants treated with native IAA (set 'b') and IBA (set 'c') were kept as a positive control, whereas water treated explants (set 'a') were considered as negative control. Thus, the treated explants were transferred to the culture tubes containing 15 ml solid MS medium. Each set contained 15 nos of culture tubes and inoculated tubes were kept under 16/8 h photoperiod at 25 ± 30 °C in the tissue culture chamber. The observation was made at intervals of 5, 10, 15, 20 and 25 days considering certain growth parameters such as a number of roots, the length of roots and rooting percentage and the mean ± SD data obtained from five replications. Significantly,

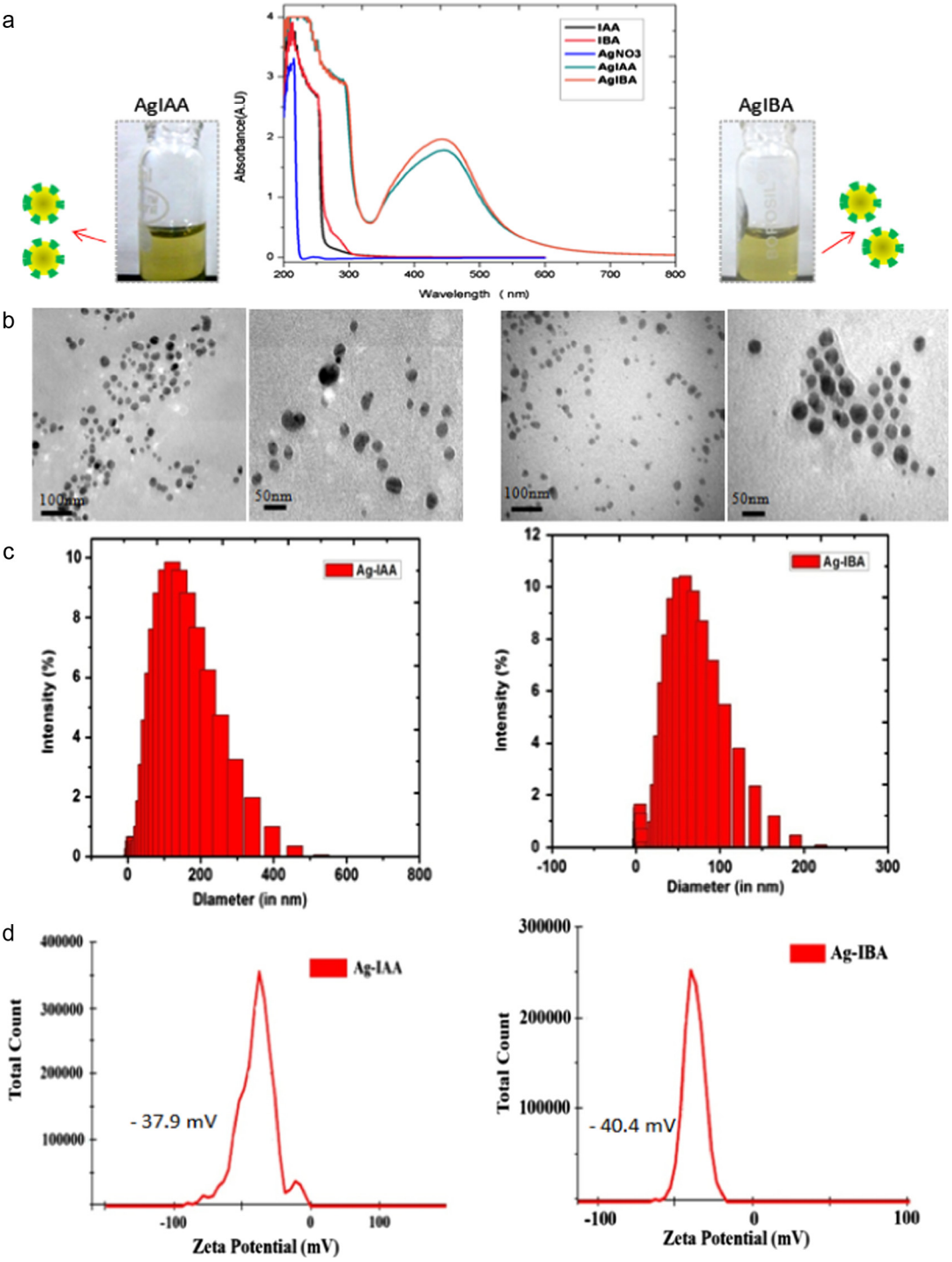

Figure 1 (a) UV-visible excitation spectral data for IAA, IBA, $AgNO_3$, AgIAA and AgIBA. (b) Transmission electron microscopy images of AgIAA and AgIBA at 100 and 50 nm scales. (c) Dynamic light scattering histogram of particle size distribution corresponding to AgIAA and AgIBA. (d) Zeta potential measurement for AgIAA and AgIBA.

the uptake, distribution and bioaccumulation of hormone-stabilized AgNPs in the treated plant cultures of *N. tabacum* were studied through UV absorbance and fluorescence spectrometry (Horiba fluoromax 4, Japan), Inverted microscopy (RTC /7a, Radical, India) and SEM-EDS (scanning electron microscopy coupled with energy dispersive spectroscopy, Hitachi SU600) respectively. Initially, uptake phenomena were studied and recorded through UV Spectrum absorbance by *N. tabacum* explants incubated with one of the hormones stabilized nanoparticles (AgIAA) for 0,10,20 and 30 min. And the distribution of hormone AgNPs in the treated plant tissue was studied because of indole derivatives of IAA and IBA intrinsic fluorescent property (Cristina et al., 1998; Sanchez et al., 1991). It was confirmed by a simple method using UV light illumination by exposing, five non-fluorescent plastic Eppendorf tubes containing water, IAA, IAA-AgNPs, IBA and IBA-AgNPs. For fluorescence spectrometry, solutions of native IAA and IBA, AgIAA and AgIBA were used for fluorescence analysis at RT. For inverted microscopic analysis, samples of hormone AgNPs treated plant tissues were taken from the apical and basal parts after 48 h culture and it was fixed in glass slide with ddH_2O, and here sections of samples were obtained through hand-cut. Moreover, bioaccumulation factor (BAF) of silver element studied in the treated plant from the microtome sectioned samples by SEM-EDS (scanning electron microscopy coupled with energy dispersive spectroscopy) analysis. In order to assess the possible phytotoxicity of hormone AgNPs treated plants, studies were done through morphological appearance and molecular level mutations by RAPD markers. RAPD a predominant technique has been used to reveal DNA damage or molecular alterations at any range in plant gene reported previously (Dwivedi et al., 2000; Tingey et al., 1993; Arulbalachandran et al., 2009). From RAPD analysis, genomic DNA was extracted from leaves of all the treated *in vitro* cultured microcuttings using the standard procedure (Dellaporta et al., 1983). Using RAPD decamer (OPK-7), the DNA samples were screened and selected for further analysis based on its ability to produce multiple banding patterns of PCR amplified products. The reactions were carried out in a DNA-gradient thermocycler (Peltier thermocycler model L196GGD, Lark Innovative Technologies, India) with standard amplification protocol (Sambrook and David Rusell, 1989). After the reaction was completed, PCR-amplified products were subjected to 2% agarose gel electrophoresis. Further, the gel product was analyzed in a UV transilluminator and the picture was photographed. Based on *in vitro* results, *ex vitro* application was designed and performed.

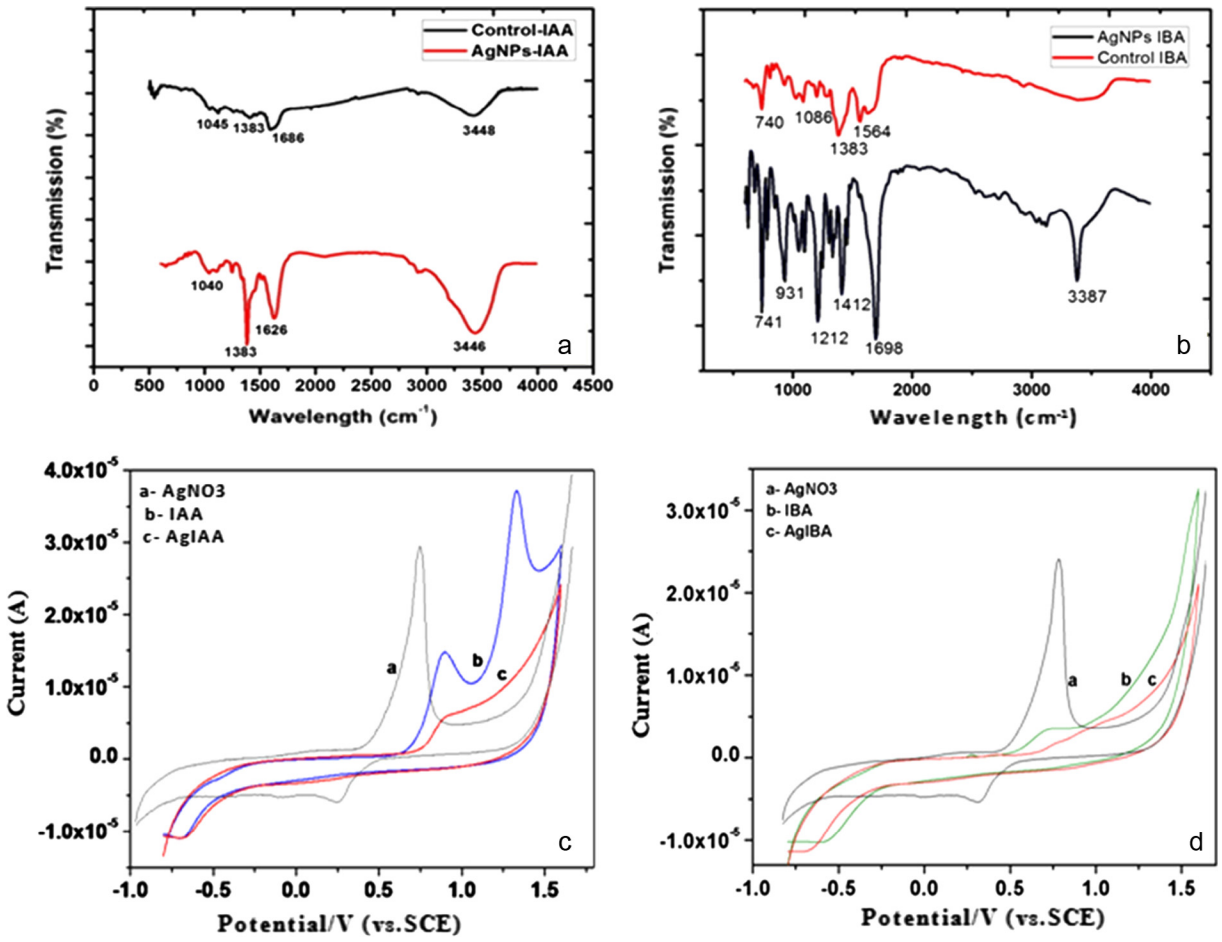

Figure 2 (a) Fourier transform infrared overlaid spectra of native IAA and AgIAA and (b) native IBA and AgIBA, (c) cyclic voltammograms of IAA and (d) IBA reduced AgNPs: Curve-a: are $AgNO_3$, Curve-b: are pure rooting hormones of both IAA and IBA, Curve-c: are reduced form of AgNPs by both rooting hormones.

2.5. Ex vitro application and assessment of IAA- and IBA-stabilized AgNPs on stem cuttings

The present investigation deals with the *ex vitro* assay to assess both rooting ability and antifungal activity (indirect & direct) of the IAA- and IBA-stabilized AgNPs. Fungal strains of *Curvularia lunata, Rhizoctonia solani* and *Colletotrichum gloeosporioides* were obtained from Plant pathology laboratory, Center for advanced studies in Botany, University of Madras. The three fungal conidial suspensions (10^6 conidia/ml) of the organisms were prepared in sterilized distilled water for 10-day old cultures. Freshly prepared suspension of inoculum from three cultures was mixed and 1 ml of pooled inoculums was inoculated into each plastic cup containing sterilized moistened soil with inside volume of 250 ml. Stem cuttings of *Hibiscus rosa sinensis* were collected from the youngest available woody stems in the vicinity of our university campus. Following tip cutting method, stems of 10–12 cm long were detached with 0.7–1.0 cm diameter and 2–3 nodes without adult leaves were obtained. For this study, we have taken six sets and each set contains four stem cuttings accordingly to be treated with IAA- IBA-capped AgNPs (approximately 0.02 mg/ml), native IAA-IBA (10 mM) test solutions and both 1% bavistin (systemic fungicide) and water treated kept as positive and negative controls. Each set of cuttings was soaked (basal long soak method) for 30 min with its respective solution. After treatment, the cuttings were tapped slightly to remove excess solutions and inserted one each into phytopathogenic fungi inoculated soil at 2.5 cm deep inside. The plastic cups with cuttings were kept in a tray chamber with translucent polyethylene enclosed in a glass-house. Either side of the tray chamber was left open during the day to prevent excessive heat build-up. No supplemented illumination was provided except on cloudy days. Water was sprinkled once daily depending upon the soil moisture status. Holes in the bottom of the cups allowed excessive water drainage. The cuttings were examined for adventitious root initiation and disease progress at 30th day and the data were recorded. The disease progress is assessed throughout the experiment by observing the roots, stems and leaves by discoloration and bodily damage. The results were expressed as mean values ± standard deviations (S.D.) from the five replications. Along with this study, the hormone AgNPs mechanism of action against phytopathogens was directly assessed by the quantitative micro spectrophotometric assay (Broekaert et al., 1990) and also morphological changes were studied by simple light microscopy. In this study, centrifuged and pelleted fungal conidia from three cultures were inoculated into fresh potato dextrose broth to make conidial suspensions in the concentration of 10^6 conidia/ml. From that suspension, 100 µl of each suspensions was individually added in the 96 well microplate and incubated with 100 µl of either AgIAA or AgIBA (0.02 mg/ml) for 0–120 min at the natural light in accordance with our previously published work (Raja Muthuramalingam et al., 2015). For negative and positive controls, both water and fungicide bavistin at 1 mg/ml were used. Growth inhibition was measured at every 30 min up to 120 min on the range of 595 nm in a microplate reader. The rate of growth inhibition was determined based on the equation outlined by Broekaert et al., (1990).

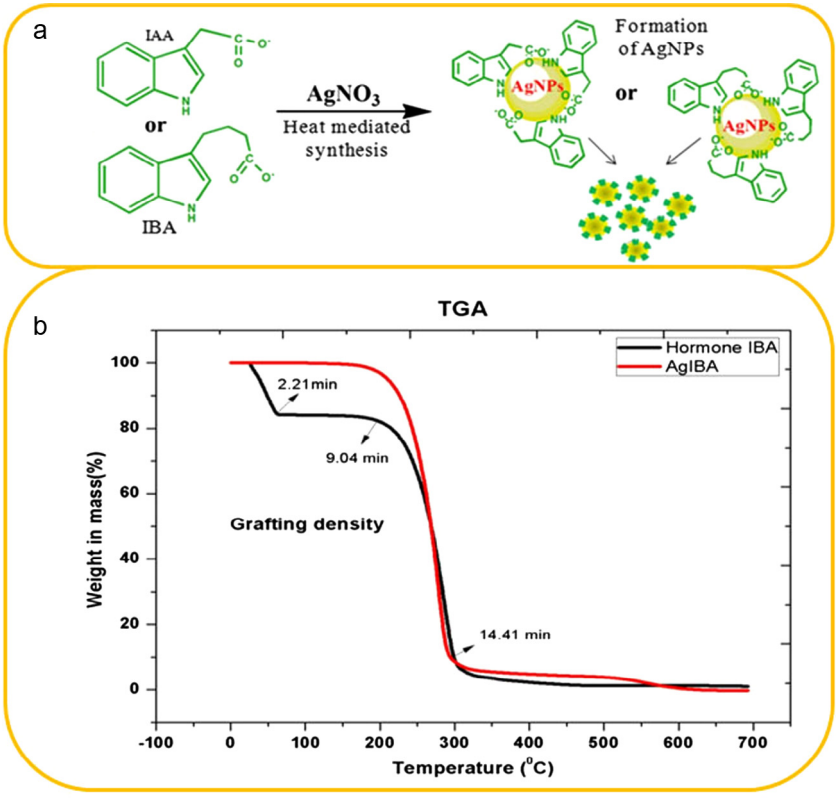

Figure 3 (a) Schematic representation of AgNPs formation by IAA and IBA root promoting hormones. (b) TGA of bare IBA hormone and AgIBA.

3. Results and discussion

3.1. Physico-chemical characteristic features of IAA- and IBA-stabilized silver nanoparticles

In Fig. 1a, UV-Vis absorption spectra for the pale yellow silver colloids obtained from both IAA and IBA prepared by heat mediated wet chemical reduction method showed a surface Plasmon absorption (SPR) band with a maximum of 450–460 nm indicating the presence of spherical and roughly spherical nanoparticles. The SPR bands of UV-Vis spectrum confirmed that the IAA and IBA hormones reduced the $AgNO_3$ to AgNPs. With standardized synthesis, both IAA- and IBA-stabilized AgNP colloids showed absorption (λ_{max}) at shorter and longer wavelength regions (above 420 nm) indicating the presence of smaller to larger particles which may be due to the complete reduction depending on rooting hormone concentration. And the calculated nanoparticles molar concentration of IAA was approximately at 5.9×10^{10} mol^{-1} (approximately 0.02 mg/ml) and for IBA it was approximately at 5.7×10^{10} mol^{-1} (0.02 mg/ml). The morphology of IAA- and IBA-stabilized AgNPs was revealed by a TEM bright field investigation. Due to sample dilution and silver containing high electron density the images were clearly captured in the TEM bright field. However, successful imaging of nanoparticles by TEM depends on the contrast of the sample relative to the background. Concentrated samples increase the contrast between the samples and surrounding could reduce the image quality. Diluted nanoparticle colloidal solution ideal for TEM analysis helps to take the desired micrograph with a large number of individual particles with good image quality. And metal nanoparticles with electron densities that are significantly higher than amorphous are easily captured by TEM including Silver, gold, copper, and aluminum ("TEM analysis of particles", 2012). In Fig. 1b, at 100 and 50 nm scales, TEM

Table 1 Effect of native auxin hormones and hormone capped AgNPs on percentage of rooting, root number and root length in treated microcuttings of *Nicotiana tabacum* model plant grown at *in vitro*. The table data represent mean ± SD values and the bar diagram for a percentage of rooting made with standard error values.

Treated with	Root numbers per explant	Root length (cm)
IAA	7 ± 0.53	1.6 ± 0.7
IBA	9 ± 0.11	2.2 ± 0.2
AgIAA	13 ± 1.1	3.6 ± 1
AgIBA	15 ± 0.3	4.1 ± 0.5
Control	0	0

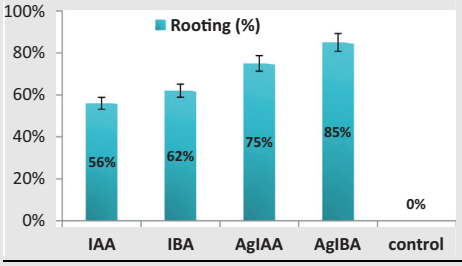

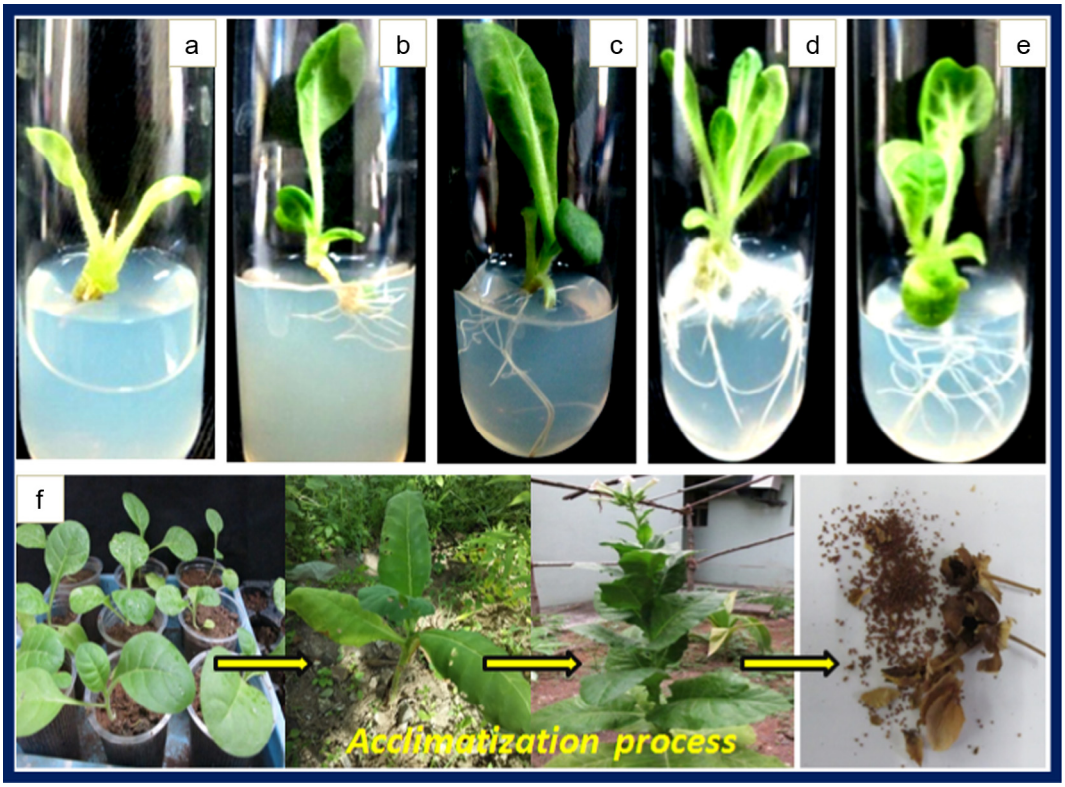

Figure 4 Rooting effect on *in vitro* cultured *Nicotiana tabacum* micro cuttings treated with: (a) control water treated, (b) IAA, (c) IBA, (d) AgIAA, (e) AgIBA and (f) acclimatization stages of hormone AgNPs treated plants.

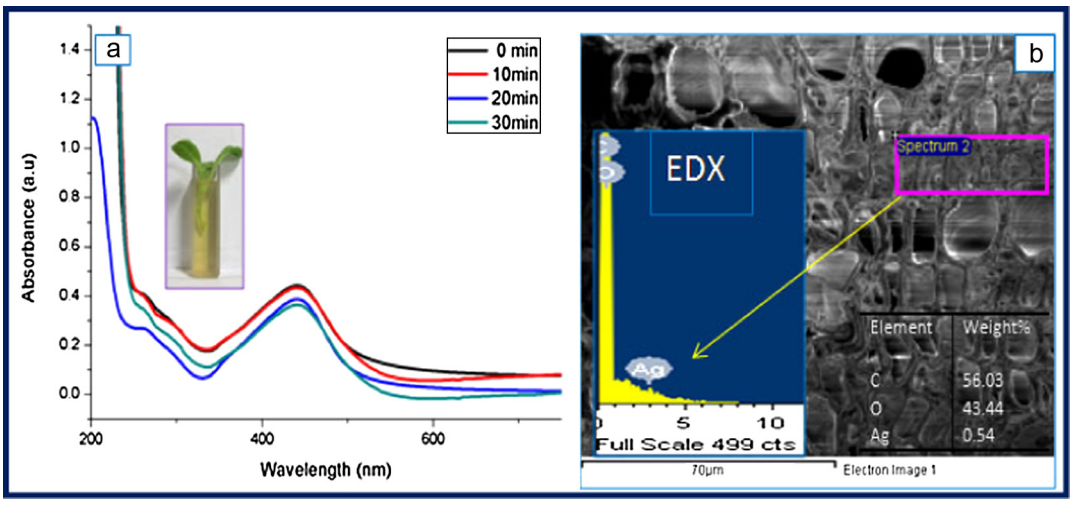

Figure 5 (a) UV absorbance spectrum of hormone AgNPs (AgIAA) taken into the plant microcuttings at 0–30 min. (b) SEM-EDS analysis of BAF (bioaccumulation factor) into hormone AgNPs treated plant shows Ag element X-ray excitation peak with the weight of 0.54%.

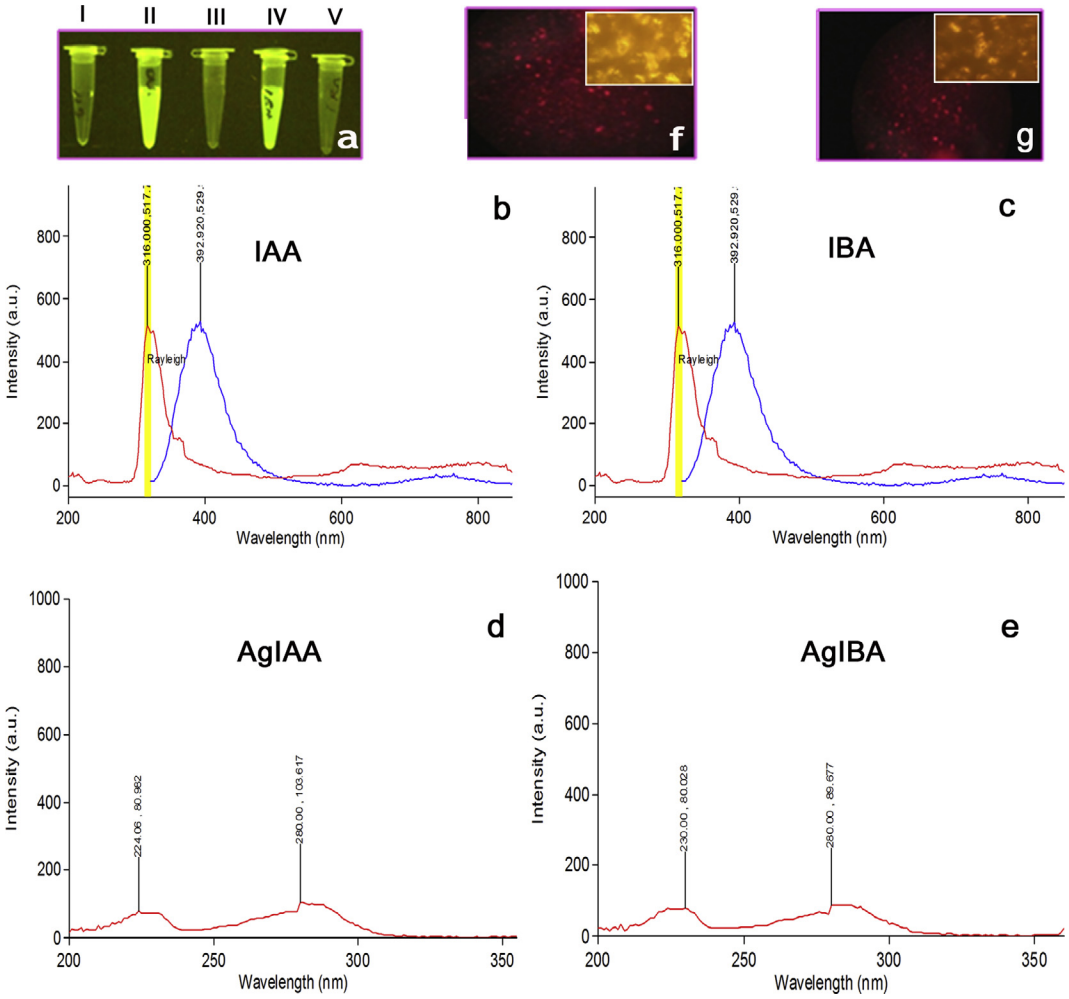

Figure 6 Uptake and location of hormones AgNPs into treated *Nicotiana tabacum* micro cuttings studied by fluorescence methods: (a) UV light exposure to (I) water (II) IAA (III) AgIAA (IV) IBA (V) AgIBA; fluorescence spectrum analysis of excitation and emission of (b) IAA (c) IBA (d) AgIAA (e) AgIBA; fluorescence spots inside the plant tissue treated with (f) AgIAA and (g) AgIBA.

images show the presence of uniform spherical shaped and monodispersed IAA- and IBA-stabilized silver nanoparticles in the size range of 20–150 and 6–70 nm, respectively. The pale yellow color of the solution mainly depends on the size of colloidal silver within the range of 10–150 nm. In agreement with that statement and TEM results, Fig. 1c of DLS analysis histograms of IAA-stabilized AgNPs showed that it has distributed particle ranges from 20 to 140 with the average size of 97.35 nm in diameter and IBA-stabilized AgNPs have distributed particle size ranges from 4 to 65 nm with the average size of 44.17 nm in diameter. The peak intensity indicates the multiple populations of spherical particles of diameter present in both of silver colloidal solutions. Electric potentials at the boundary of nanoparticles were examined by Malvern instrument, the mean zeta potential of IAA-stabilized AgNPs was −37.9 mV and that of IBA capped AgNPs was −40.4 mV (Fig. 1d). It concluded that both particles in colloidal solution attained overall surface negative charges which give opposite electrostatic repulsion between particles which was responsible for particle dispersion. Therefore, nanoparticles with zeta potential value greater than +25 mV and less than −25 typically have the high degree of stability. Indeed, hormone-stabilized AgNPs have greater stability up to 6 months at RT examined by UV-Vis spectra (data not shown). FTIR analysis was carried out to understand the interaction of IAA and IBA functional group with silver nanoparticles. Fig. 2a shows FTIR overlapped spectra of IAA and IAA-stabilized AgNPs. Spectra peak at 1045 and 1383 cm^{-1} assigned to HC═CH, CH═CH stretches of the aromatic ring. The peak at 1686 cm^{-1} corresponds to the carbonyl group (C═O) or C═C stretch and peak at 3448 cm^{-1} was assigned to ═OH group of IAA. After the synthesis of AgNPs using IAA, FTIR spectral peaks were found to shift toward shorter wavelength with higher intensity and sharp band. Particularly, peaks at 1383, 1625 and 3446 cm^{-1} were found with increased intensity than IAA spectra. Small peak shift at 3448–3446 cm^{-1} and significant shift at 1686–1625 cm^{-1} were observed and these peak shifts were mainly due to the interaction of carbonyl and carboxyl groups with silver nanoparticles. Similarly, in Fig. 2b, FTIR spectra of indole 3-butyric acid show a broad peak at 3400 cm^{-1} which corresponds to OH group and peaks at 1086 and 1383 cm^{-1} were assigned for C═C and C═C stretch of the aromatic ring with the carbonyl group corresponding to peak at 1564 cm^{-1}. IBA capped silver nanoparticles show FTIR transmittance peaks shift toward long wavelength with increased intensity. Specifically, peaks at 1212, 1412, 1698 and 3387 cm^{-1} correspond to IBA aromatic ring, carbonyl, and hydroxyl groups, respectively. These peak shifts and increased intensity of FTIR spectra are mainly due to the interaction of carboxyl and hydroxyl group of IBA with silver nanoparticles. It is clearly evident that carboxyl/ hydroxyl functional groups of IAA and IBA were involved in the reduction of silver ion in Ag metal and also acted as capping agent to control the nucleation growth in silver nanoparticles synthesis (Wade, 2003). Cyclic voltammetry is generally used to study the electrochemical properties of an analyte in solution. The redox potential of silver ions to AgNPs in the presence of rooting hormones in solution is verified by CV. Fig. 2c and d shows the cyclic voltammograms of $AgNO_3$, IAA and IBA, IAA- and IBA-stabilized AgNPs using platinum electrode with the fresh surface in LiClO4 (0.1 M) supporting electrolyte, at a scan rate of 100 mV/s. In Fig. 2c and d, an aqueous solution of $AgNO_3$ (curve a) exhibits one reduction peak at +0.27 V and a larger oxidation peak centered at +0.71 V in the potential range between −1 and +1.5 in both. The reduction peak is attributed to the electrodeposition of silver ions on the electrode surface, and the oxidation peak corresponds to the oxidation of silver from the electrode. In Fig. 2c and d, native IAA (curve b) exhibited no reduction peak and two oxidation peaks were observed at +0.92 V and +1.32 V in the aqueous medium. And native IBA exhibited no reduction peak and small oxidation peak at +0.72 V. Fig. 2c and d of (curve c) exhibits a complete reduction of the Ag^{+} ions to Ag° by IAA and IBA to AgNPs was indicated by the absence of cathodic and anodic peak current by $AgNO_3$ ions as shown in curve c. The reduction of AgNO3 may be due to the transfer of electrons from the IAA and IBA containing carboxyl/hydroxyl group to a metal ion, and the resulting AgNPs were stabilized. In Fig. 3a, we exhibit the scheme of AgNPs synthesis correlated with FTIR and CV analytical results. TGA also confirmed the presence of hormones on the silver nanoparticles as evidenced by a 94% weight loss corresponding to the grafted hormones at 300 °C. From TGA results, the hormone started denatured at 100 °C and completely denatured at 300 °C in 14.41 min. Hormone IBA synthesized Silver nanoparticles possessed 6% remain at the 300 °C in 14.41 min which concluded that 94% of hormone (Fig. 3b) was grafted on nanoparticles and the grafting density was also calculated using these data according to Benoit et al., (2012). The data revealed that 10,940 units of IBA chain are grafted on one particle and the density of hormone IBA unit in one particle is calculated as 17 unit/nm^2.

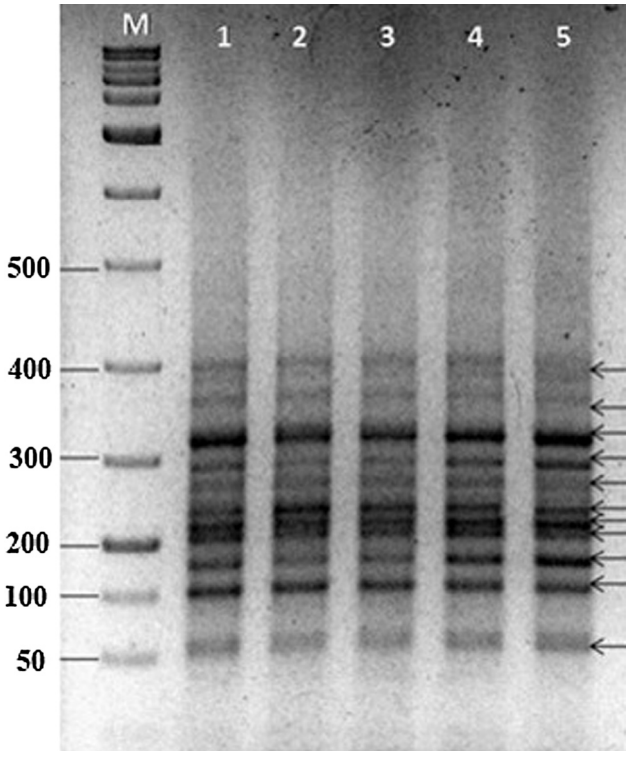

Figure 7 RAPD profile of *in vitro* treated plants: M - 100 kb Marker, Lane 1 - control, Lane 2 - IAA treated, Lane 3 - IBA treated, Lane 4 - AgIAA treated and Lane 5 - AgIBA treated.

3.2. The effect of IAA-and IBA-stabilized AgNPs on in vitro treated micro cuttings

The result was obtained after the 25th day from the inoculation of basal dipped micro cuttings cultured on MS medium. Astonishingly, the visual and statistical analysis determined that hormone AgNPs proved as a potential root enhancer compared to native hormone-treated *N. tabacum* micro cuttings. Fig. 4d and e shows the highly promoted rhizogenic effect of IAA- and IBA-stabilized AgNPs treated plants, and it has two- and threefold higher stimulated root numbers and root hairs with elongated roots than native IAA and IBA hormone-treated plants (Fig. 4b and c). A negative control plant showed no sign of root initiation and two stunted leaves were observed in the nodal region as shown in Fig. 4a. From the treated plants, adventitious roots arose from the cambium nearby the mechanically damaged stem tissue at micro cuttings. The mean data of root numbers and length of roots were calculated and are represented in Table 1 with a bar graph of rooting percentage. This attempt with both IAA- and IBA-stabilized AgNPs, is certainly a successful one which was critically relevant to increase the root growth of *in vitro* cultured treated shoots compared to conventional native hormones treated. These results also pave the way to *ex vitro* studies in similar treatment method. The UV-Vis spectrometry analysis has given some potential information regarding hormone nanoparticles absorption into the treated plant. In Fig. 5a spectrum data show that absorbance intensities were

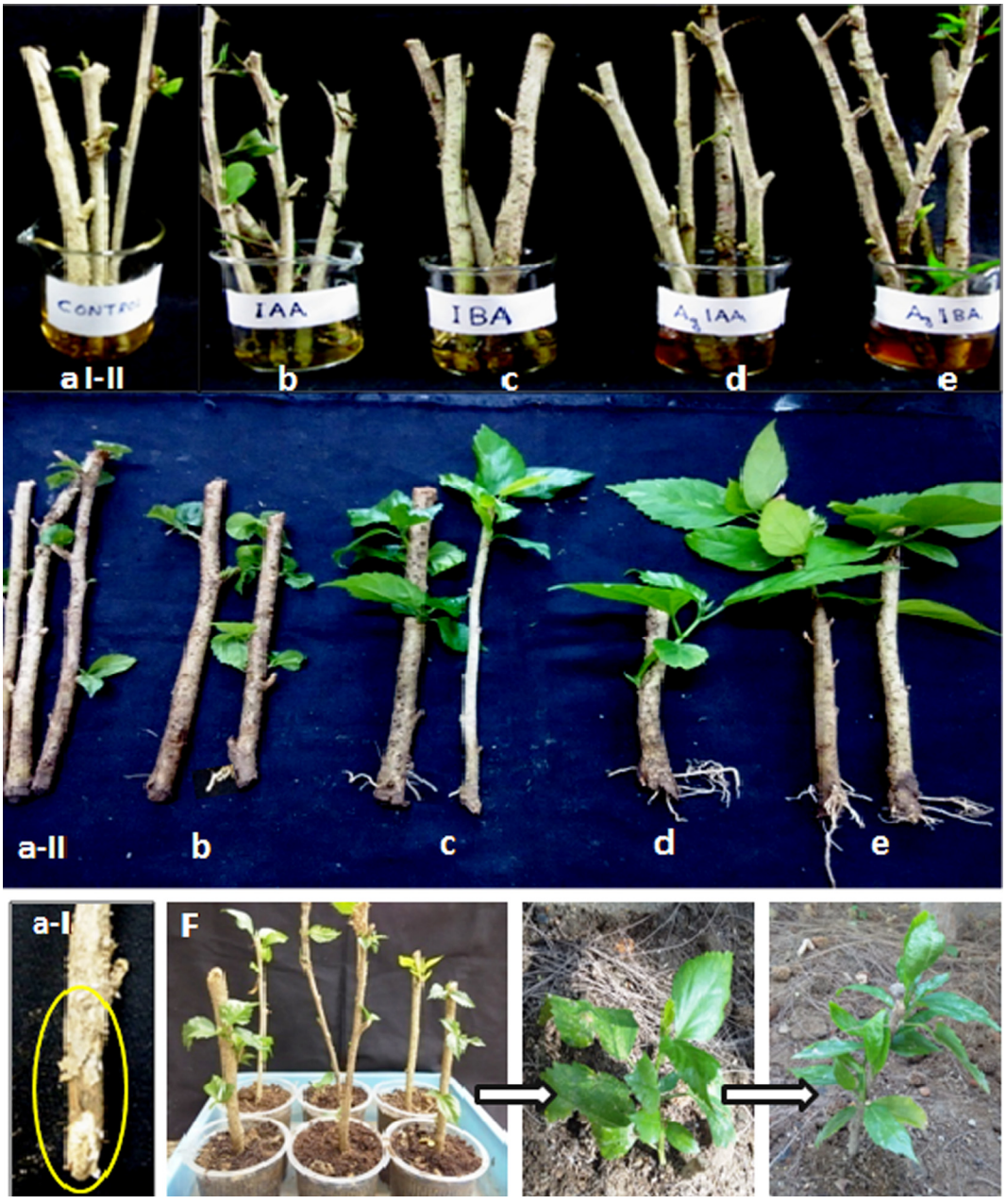

Figure 8 Rooting effect on *ex vitro* cultured *Hibiscus rosa sinensis* stem cuttings treated with: (a) I & II-water and bavistin fungicide treated as controls, (b) IAA, (c) IBA, (d) AgIAA, (e) AgIBA and (f) Acclimatization stages of hormone AgNPs treated plants.

decreased when the micro cutting incubated at 0–30 min with AgIAA. According to Mie theory calculation through absorbance intensities, during 30 min incubation, only 2% of hormone nanoparticles (AgIAA) was taken by micro cuttings revealed. It may vary by long time incubation and the size of the micro cuttings used to treat. The distribution of nanoparticles into treated plants was studied based on auxin hormone fluorescence properties, such that it is exposed to UV light, the native IAA and IBA hormones exhibited fluorescence, but IAA- and IBA-stabilized AgNPs did not have fluorescence (Fig. 6a). It assures that the time of AgNPs formation had quenched the fluorescence indole derivatives of native IAA and IBA through molecular energy transfer which was also confirmed by fluorescence spectrometry. In Fig. 6b, fluorescence spectra reveal that the wavelength at 364 nm native IAA exhibited excitation spectra at 316 nm and emission spectra at 392 nm with strong intensity level. IAA-stabilized AgNPs have excitation spectra at 224 nm and emission spectra at 280 nm with very low intensity (Fig. 6d). The native IBA also has exhibited excitation spectra at 324 nm and emission spectra at 404 nm with strong intensity level, but IBA-stabilized AgNPs exhibited decreased fluorescence intensity peak because of the static quenching of IBA fluorescence (Fig. 6c and e). This type of quenching requires molecular contact between fluorophore and quencher. Here Ag^+ ions were employed as a quencher during the formation of AgNPs where the energy was transferred from fluorophore of hormone molecules. At this point, we anticipated the real fact of hormone-stabilized nanoparticles inside the treated plants. By inverted microscope analysis using the green excitation filter at 250–400 nm, we explored fluorescence spots inside the basal region not at the apical region in both the hormone-stabilized AgNPs treated plant specimen illustrated in Fig. 6f and g. The possibility of fluorescence of AgNPs treated plant might be the interaction between AgNPs and plant tissue. These interactions might lead to intracellular uptake, and for their part the biomolecules might induce phase transformations, free energy releases, restructuring and dissolution of hormone capped nanomaterial. Generally in a plant, uptake and accumulation occur only during the initial time of treating in an early pulse in the surrounding tissue at wounding region and were the sole reason for apical part not possessing fluorescence (Bennett et al., 1996). The kinetics of the AgNPs uptake of solution have been determined by its nanoscale range, which mimics like inorganic nutrient molecules could be easily actively transported through vascular structures of the plant at the wounding region. The SEM-EDS elemental analysis also revealed the presence of Ag metal elements in treating plant tissue and the bioaccumulation concentration of silver was detected by EDS only in trace level (0.54%) Fig. 5b. With this significant analysis, we also evidenced no morphological damages and growth inhibition like metal induced stress was observed in hormone-stabilized AgNPs treated plants. In RAPD analysis, the fluorogram of agarose gel banding pattern of PCR amplified fragments also reveals that no banding variation (0%) or no mutation at the DNA level between controls and both hormone-stabilized AgNP treated plants was observed (Fig. 7). Therefore, it is assumed that silver ion, a non-essential metal ion for plant growth either may have a role in plant growth or may have inhibited any complexes which involve a negative role in plant growth. Additionally, there are some precedential reports saying that Ag^+ is able to promote rooting alone, without an addition of auxins to *in vitro* culture mediums (Kumar et al., 2009). All plants possess a certain tolerance to heavy metals, but at exceeded concentration and prolonged exposure to silver metal and any other metals definitely can cause toxic effects and disorder such as transpiration and photosynthesis inhibition, disturbance of metabolism and oxidative stress, all of which collectively yield a common effect on plant development and growth. Contrary to our results, we produce several lines of evidence that suggest the involvement of silver nanoparticles as a carrier of rooting hormone to deliver into the plant for the root development. Successful *in vitro* rooted plants treated with AgNPs were transferred to the culture tray containing soil then kept in the greenhouse. After one month of transformation, the *N. tabacum plants* were sustained by stimulated root growth and further planted in the field. The AgNPs treated field-grown plants have 90% of the success rate of acclimatization and completed its cycle after 4 months of producing viable seeds (Fig. 4f). Therefore, the hormone-stabilized AgNPs promoted the roots fully functional even after transfer to soil and very well acclimatized like normal plants.

3.3. Effect of IAA- and IBA-stabilized AgNPs on ex vitro shoot cuttings

In this research work, rooting ability and antimicrobial activity (indirect and direct) of rooting hormone synthesized silver nanoparticles were investigated. After 30 days of surveillance, only those stem cuttings exogenously treated with native hormones and hormone capped AgNPs survived and regenerated. After 45 days of examination of cuttings, highest root number with elongated roots was observed only in AgIBA treated cuttings and AgIAA treated showed one fold reduced growth than AgIBA treated (Fig. 8d and e). Also, differences were observed between these two native hormones-treated plants shown in Fig. 8b and c. Both IAA and IBA native hormones treated showed a very low number of roots with short lengths.

Table 2 Effect of native auxin hormones and hormone capped AgNPs on percentage of rooting, root number and root length in treated stem cuttings of *Hibiscus rosa sinensis* model plant grown at *ex vitro*. The table data represent mean ± SD values and the bar diagram for a percentage of rooting made with standard error values.

Treated with	Root numbers per explant	Root length (cm)
IAA	1 ± 0.2	1 ± 0.3
IBA	1 ± 0.13	1.2 ± 0.55
AgIAA	7 ± 0.44	2.2 ± 1
AgIBA	9 ± 0.3	3.1 ± 1.2
Control	0	0

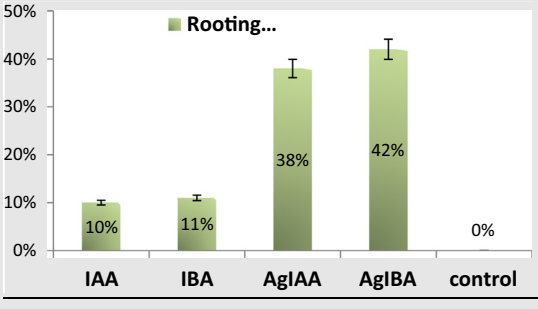

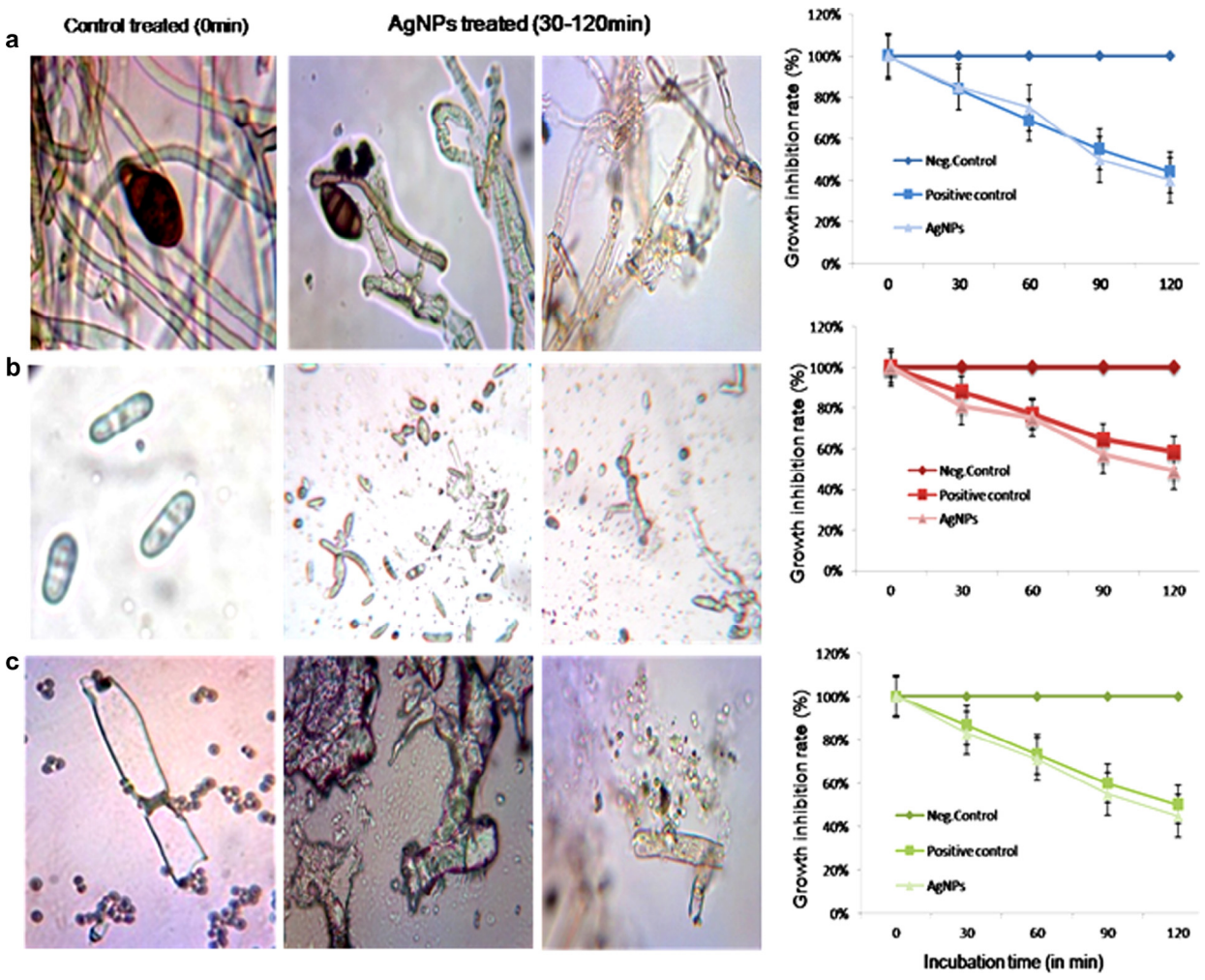

Figure 9 Direct antifungal activity of Hormone stabilized AgNPs: Light microscopic images of (a) *Curvularia lunata,* (b) *Colletotrichum gloeosporioides* and (c) *Rhizoctonia solani* with control water and hormone AgNPs treated. Subset of chart shows growth inhibitory percentage obtained from micro spectrophotometric assay to the corresponding organism treated with AgNPs. Data were calculated by mean ± SD and presented in a chart.

The detailed statistical data are expressed in Table 2. A timely comparison observed between *in vitro* and *ex vitro* native hormones treated, and *ex vitro* cuttings seems that root growth was inhibited by soil inoculated pathogens. Thus, pathogens might limit the nutrient uptake and water potential which were important for root growth. And the bavistin (positive control) treated did not show any root initiation, and after 40 days they started to dry and were finally lost (Fig. 8a-II). However, there was no visual evidence of inhibition of root development and were symptoms of soil inoculated pathogens in all treated stem cuttings except water (negative control) treated. It has some visual damping off and canker disease symptoms at the base of stem cuttings which were common symptoms for *Rhizoctonia solani* and *Curvularia lunata* (Fig. 8a-I). So it was determined that direct application of hormone-stabilized AgNPs at the base of root cuttings was an effective way to protect the cuttings from pathogen invasion. Through obtaining knowledge from *in vitro* study, we could firmly spell that basal end treated with hormone-stabilized nanoparticle has accumulated in the treated area and slowly gets oxidized to release rooting hormone and silver ion which facilitates prolonged root promoting activity and protects root inhibition activity from soil inoculated phytopathogens. It is concluded hormone capped silver nanoparticles have best inhibitory properties compared to fungicides against root disease causing pathogens and sustained with their potentiality to promote the root growth on treating *Hibiscus* stem cuttings. The percentage of the acclimatization rate of AgNPs treated (93%) was also higher than native hormone treated (47%). As per earlier reports, hormone IBA is an effective rooting hormone than IAA by many studies (Stefancic et al., 2005), such a way that, we achieved similar results from both *in vitro* and *ex vitro* studies. Here hormone-stabilized AgNPs especially Ag-IBA have better activity than Ag-IAA and native IAA, and IBA was confirmed through many observations. The direct antifungal assay and the micro spectrophotometric assay quantitatively revealed the inhibitory action of AgNPs against three plant pathogens of *Curvularia lunata, Rhizoctonia solani and Colletotrichum gloeosporioides*. The AgNPs (AgIBA) show better activity with various growth inhibition rates compared to controls (Fig. 9). And the light microscopic observations of direct antifungal activity have clear evident that all the three strains

were very much susceptible to hormone AgNPs. It is observed disrupted cell structures and cellular leakage are due to its highly reactive potential activity (Fig. 9). Regarding phytotoxicity of hormone AgNPs, significantly, there were no morphological damages at treated plants. As far as propagation work is concerned, once the process and influence of hormone-stabilized nanoparticles are well understood, it should be possible to improve techniques considerably, thus enabling work to proceed with more confidence and with greater certainty of success in agriculture.

4. Conclusion

Poor rooting is a major problem with horticulture plants and it has vast economic consequences with losses estimated at 10–25% with nursery crops and 5% with ornamental crops at every year all over the world. The administration of auxin hormones to induce rooting of root cuttings has early established a method to achieve rooting. Though, this method often fails and other rooting treatments are not available because it has been employed more than 60 years without any technology advancements and alternatives. Hence, a nanotechnology to biotechnological approach, very first time we achieved in the synthesis of AgNPs using auxin hormones and satisfactorily confirmed its physiochemical properties through various sophisticated instrumental analyses. The hormone stabilized nanoparticles, as "nanobullets" have got real potential actions which were proved in both *in vitro* and *ex vitro* studies by enhanced root growth and root numbers compared to control auxin hormones (IAA, IBA) treated. In *ex vitro* studies, "nano carrier" has rendered good defense over the invasion of root inhibitory soil pathogens by its known silver antimicrobial activity. It is also determined by the direct antifungal assay performed against destructive three plant pathogens. Significantly, the outcome of absorption, distribution and bioaccumulation studies of "nanobullets" in the treated plant tissues clarifies the real kinetics of hormone AgNPs to the treated plant specifically inside the cell. Moreover, targeted and slow release of the "nanobullets" could reduce the net amount of hormone and silver accumulation which could minimize the adverse effects on plant also proved by RAPD molecular markers. This finding determined the potentiality of "nanobullets" may increase rooting on species or varieties that are difficult to propagate shoot cuttings in nurseries. Hence, this is an innovative strategy in the technology advancement than existing conventional rooting hormone application which will calibrate directly on the target rather than reach the soil in large quantities. Through the experimental analysis also, we can firmly say that within the cost of markedly available rooting enhancer (275 ml) we can economically produce more than 50 l of "nanobullets" which can be stable for few months to use. Besides being economically sound, a management strategy should also be simple, safe, inexpensive to apply, and sufficiently effective to reduce diseases to acceptable levels. This work might be an initial step in the milestone of nanobiotechnological revolution which is also yet to firmly establish its roots into an agricultural field.

Acknowledgment

We, authors, thank University Grand Commission of India sponsored National Centre for Nanoscience and Nanotechnology, the University of Madras for Instrumentation facilities.

References

An, J., Zhang, M., Wang, S., Tang, J., 2008. Physical, chemical and microbiological changes in stored green *Asparagus* spears as affected by coating of silver nanoparticles. PVP-Food Sci. Technol. 41, 100–107.

Arulbalachandran, D., Mullainathan, L., Karthigayan, S., Somasundaram, S.T., Velu, S., 2009. Evaluation of genetic variation in mutants of Black gram (*Vingna mungo (L.) Hepper*) as revealed by RAPD markers. Emir. J. Food. Agric. 21 (2), 42–50.

Battke, F., Leopold, K., Maier, M., Schidhalter, U., Schuster, M., 2008. Palladium exposure of barley uptake and effects. Plant Biol. 10, 272–276.

Becker, D., Hedrich, R., 2002. Channeling auxin action: modulation of ion transport by indole-3-acetic acid. Plant Mol. Biol. 49, 349–356.

Bennett, M.J., Marchant, A., Green, H.G., May, S.T., Ward, S.P., Millner, P.A., Walker, A.R., Schulz, B., Feldman, K.A., 1996. Going the distance with auxin: unravelling the molecular basis of auxin transport. Science 273, 948–950.

Broekaert, W.F., Terras, F.R.G., Cammue, B.P.A., Vanderleyden, 1990. An automated quantitative assay for fungal growth inhibition. J. FEMS Microbiol. Lett. 69, 55–60.

Craig, M., Jason, C.W., 2011. Toxicity of silver and copper to *Cucurbita pepo*: differential effects of nano and bulk-size particles. Environ. Toxicol., 26

Cristina, S.R., Miqual, A.Q., Martin, J.B., Victoria, V., Antonio, H., 1998. Improved procedure to determine indole-3-acetic acid by fluorescence derivatives. Phytochemistry 27 (6), 1579–1581.

Dellaporta, S.L., Wood, J., Hick, J.B., 1983. A plant DNA mini preparation; version II. Plant Mol. Biol. Rep. 1, 19–21.

Benoit, Denise N., Zhu, Huiguang, Lilierose, Michael H., Verm, Raymond A., Ali, Naushaba, Morrison, Adam N., Fortner, John D., Avendano, Carolina, Colvin, Vicki L., 2012. Measuring the grafting density of nanoparticles in solution by analytical ultracentrifugation and total organic carbon analysis. Anal. Chem. 6,84 (21), 9238–9245.

Dwivedi, S.L., Gurtu, S., Chandra, S., Yuejinand, W., Nigam, N., 2000. Assessment of genetic diversity among selected ground nut germplasm: RAPD analysis. Plant Breed. 120, 345–349.

El Sayed, M.E., 2004. Shape-dependent catalytic activity of platinum nanoparticles in colloidal solution. Nanotechnol. Nanotechnol. 4, 1343–1348.

Sanchez, F. Garcia, Ruiz, C. Carnero, Bayona, A. Heriedia, 1991. Determination of indole-3-butyric acid in plant culture medium by fluorescence derivatization. Microchem. J. 43, 222.

George, E.F., 1996. Plant Propagation by Tissue Culture, Part 2. In Practice. Exegetics Ltd., Eddington.

Ghodake, G., Seo, Y.D., Lee, D.S., 2011. Hazardous phytotoxic nature of cobalt and zinc oxide nanoparticles assessed using *Allium cepa*. J. Hazard. Mater. 186, 952–955.

Priede, Gunta, Klavina, Dace, 2011. In vitro cultivation and root initiation of the endangered plant *Pulsatilla patens*. Environ. Exp. Biol. 9, 71–74.

Salama, M.H. Hediat, 2012. Effects of silver nanoparticles in some crop plants, common bean (*Phaseolus vulgaris L.)* and corn (*Zea mays L.*). Int. Res. J. Biotechnol. 3 (10), 190–197.

Lian, Hong-Yuan, Hu, Ming, Liu, Chia-Hung, Yamauchi, Yusuke, Wu, Kevin C.-W., 2012. Highly biocompatible, hollow coordination polymer nanopartices as cisplatin carriers for efficient intracellular drug delivery. Chem. Commun. 48, 5151–5153.

Ahmed, Iftikhar, Iram, Shazia, Cullum, John, 2005. Genetic variability and aggressiveness in *Curvularia lunata* associated with rice-wheat cropping areas of Pakistan. Pak. J. Bot. 38 (2), 475–485.

Juhel, G., Batisse, E., Hugues, Q., Daly, D., Van Pelt, F.N.A.M., O'Halloran, J., Jansen, M.A.K., 2011. Alumina nanoparticles enhance growth of *Lemna minor*. Aquat. Toxicol. 105, 328–336.

John Lockwood, L., 1985. Soil borne plant pathogens: concepts and connections. In: Presidential Address, 77th Annual Meeting, The American Phytopathological Society.

Jones, P.A., 2006. Nanotech revolution in agriculture and the food industry. Inform. Syst. Biotechnol. <http://www.isb.vt.edu/articles/jun0605.htm>.

Wu, Kevin C.-W., Yang, Ya-Huei, Yang, Yung-He, Liang, Yung-He, Chen, Hui-Yuan, Sung, Eric, Yamauchi, Yusuke, Lin, Feng-Huei,

2011. Facile synthesis of hollow mesoporous hydroxyapatite nanopartilces for intracellular bio-imaging. Curr. Nanosci. 7 (6), 926–931.

Khan, M.R., Ashraf, S., Rasool, F., Salati, K., Mohiddin, F.A., Haque, A., 2014. Field performance of Trichoderma species against wilt disease complex of chickpea caused by *Fusarium oxysporum*, *F. sp. ciceri* and *Rhizoctonia solani*. Turk. J. Agric. Sci. 38, 447–454.

Mariya, K.V., Mohamed, H., 2014. Nanoparticles and plants: from toxicity to activation of growth. Handbook Nanotoxicol. Nanomed. Stem Cell Use Toxicol..

Monica, R.C., Cremonini, R., 2009. Nanoparticles and higher plants. Caryologia 62, 161–165.

Zakaria, Mohammed B., Belik, Alexei A., Liu, Chia-Hung, Hsieh, Han-Yun, Liao, Yu-Te, Malgras, Victor, Yamauch, Yusuke, Wu, Kevin C.-W., 2015. Prussian blue derived nanoporous iron oxides as anticancer drug carriers for magnetic-guided chemotherapy. Chem. Asian J. 10, 1457–1462.

Murashige, T., Skoog, F., 1962. A revised medium for rapid growth and bioassays with tobacco tissue cultures. Physiol. Plant. 15, 473–497.

Paramelle, D., Sadovoy, A., Gorelik, S., Free, P., Hobley, J., Fernig, D.G., 2014. A rapid method to estimate the concentration of citrate capped silver nanoparticles from UV-visible light spectra. Analyst 139, 48–55.

Perea de Lugue, A., Rubiales, D., 2009. Nanotechnology for parasitic plant control. Pest Manage. Sci. J. 65 (5), 540–545.

Raja Muthuramalingam, T., Chandrasekar, S., Dharanivasan, G., Nallusamy, D., Rajendran, N., Kathiravan, K., 2015. Bioactive bile salt capped silver nanoparticle activity against destructive plant pathogenic fungi through in vitro system. RSC Adv. 5, 71174–71182.

Raqual, B., Eudald, C., Joan, C., Xavier, F., Antoni, S., Victor, P., 2009. Evaluation of the ecotoxicity of model nanoparticles. Chemosphere 75, 850–857.

Nair, Remya, Varghese, S.H., Nair, B.G., Maekawa, T., Yoshida, Y., Kumar, D. Sakthi, 2010. Nanoparticulate material delivery to plants. Plant Sci. 179, 154–163.

Samardakiewicz, S., Wozny, A., 2005. Cell division in *Lemna minor* roots treated with lead. Aquat. Bot. 83, 289–295.

Sambrook, J., David Rusell, W., 1989. Molecular Cloning: A Laboratory Manual (3). Cold Spring Harbor Laboratory Press.

Arora, Sandeep, Sharma, Priyadarshini, Kumar, Sumit, Nayan, Rajeev, Khanna, P.K., Zaidi, M.G.N., 2012. Gold nanoparticles induced enhancement in growth and seed yield of *Brassica juncea*. Plant Growth Regul. 66, 303–310.

Stefancic, M., Stampar, F., Osterac, G., 2005. Influence of IAA and IBA on root development and quality of Prunus 'GiSelA' leafy cuttings. Hort. Sci. 40 (7), 2052–2055.

Steve Dreistadt, H.D., 2001. Integrated Pest Management for Floriculture and Nurseries. UC-IPM Publication (Diseases chapter).

Transmission Electron Microscopy Analysis of Nanoparticles, 2012. NanoComposix, vol. 1.1. San Diego, CA. Retrieved from <http://www. nanocomposx.com>.

Tiberia, I.P.O.P., Pamfil, Doru, Bellini, Catherine, 2011. Auxin control in formation of adventitious roots. Not. Bot. Hort. Agro. Bot. Cluj. 39 (1), 307–316.

Tingey, S.V., Rafalski, J.A., Williams, J.S.K., 1993. In: Neff, M. (Ed.), Application of RAPD Technology to Plant Breeding. SHS Publishers, Minnesota, pp. 3–8.

Trutna, P., Liu, M., Chamberlin, D., Hadly, J., 2008. Nanoparticle measurement by spectroscopic Mie scattering. NSTI-Nanotech. 1, 834–837.

Kumar, Vinod, Parvatam, Giridhar, Ravisankar, G.A., 2009. $AgNO_3$ – a potential regulator of ethylene activity and plant growth modulator. Electron. J. Biotechnol. 12 (2), 8–9.

Wade, L.G., 2003. Organic Chemistry. Pearson Education Inc.